A98-31491 ICAS-98-2,1,3

MANUAL AERODYNAMIC OPTIMIZATION OF OBLIQUE FLYING WING

H. Sobieczky
Senior Research Scientist
DLR German Aerospace Center
Bunsenstr. 10, D-37073 Göttingen, Germany

Richard Seebass
Professor
Aerospace Engineering Sciences, CB 429, University of Colorado
Boulder, CO 80309-0429

Pei Li +
Senior Specialist Engineer
Boeing Commercial Airplane Group, P.O.B. 3707, M/S 67-LF
Seattle, WA 98124

Monika Hannemann
Computer Graphics Specialist
DLR German Aerospace Center
Bunsenstr. 10, D-37073 Göttingen, Germany

Abstract. We use a manual method and an advanced geometry generator to optimize a large wing flying obliquely at M = √2. These include the informed, but manual, design of the airfoil sections, the choice of wing planform and airfoil blending of these sections to create a wing. A manual tailoring of the wing planform and bending are used to provide a nearly elliptic load. The lift coefficient and sweep are varied sequentially to arrive at an optimum inviscid design. Considering this wing to be a flat plate, the viscous drag is computed. The altitude at which the wing enters cruise is selected to maximize L/D. This results in an Oblique Flying Wing with a viscous ML/D of 24.2, which compares well with the linear theory optimum of 25.3.

Introduction

Based on linear aerodynamic theory, the OFW warrants serious study as a large aircraft, both as a subsonic transport and as a supersonic transport. Indeed, because it is efficient at both transonic and supersonic speeds, it can provide near sonic, or slightly supersonic transport over land and supersonic transport over water, thereby increasing its productivity.

The Oblique Flying Wing (OFW), also referred to as the Oblique All Wing (OAW) to distinguish it from the Oblique Wing Aircraft (OWA), is not just the optimum aerodynamic design, it is also the optimal structural design for carrying loads, as the loads are distributed over the wing. If these loads are passengers, as distinct from cargo (or fuel in a tanker), then the minimum thickness of the wing is set by the need for aisles for the passengers.

The chord of the wing is then set by the maximum thickness-to-chord ratio achievable with an airfoil design that results in an efficient wing at the chosen flight Mach number. This is, of course, affected by sweep. Induced and wave drag are reduced by higher span and longer lengths, respectively, and thus the wing span (and length) are set by the aerodynamic efficiency required to compete with current subsonic transports. This means that as a passenger transport the OFW must be a large aircraft. We consider here the manual optimization of an 800 passenger OFW of large aspect ratio at the fixed Mach number of √2.

Supporting theories

Area Rule

The supersonic area rule, as expressed by Lomax [1], [2] tells us that the wave drag of an aircraft in a steady supersonic flow is identical to the azimuthal

+ Formerly NSF CISE Research Associate, Aerospace Engineering Sciences, University of Colorado.

average wave drag of an azimuthal series of equivalent bodies of revolution. For each azimuthal angle, the cross-sectional area of the equivalent body of revolution is given by the sum of a volume and a lift contribution.

The volume contribution is that due to a body of revolution whose cross-sectional area equals that of the cross section of the aircraft cut by the tangent to the fore Mach cone projected onto the plane perpendicular to the freestream.

The lift contribution is that due to an area distribution that equals $2\beta/q$ times the component of force on the contour cut by the fore Mach cone that lies in the azimuthal plane; this area is then projected onto the plane perpendicular to the freestream. Here β is the Prandtl factor and q is the dynamic pressure. The equivalent body of revolution due to lift thus corresponds to a body of revolution that begins at infinity with a finite "base" area (downstream or upstream). This equivalent body begins where the lift starts or ends.

Minimum Drag Bodies

The wave drag for a body of revolution of given volume and length will be a minimum if its area distribution is that of Sears [3] and Haack [4] (corrected by Sears). Thus for minimum wave drag due to volume we need a wing with a Sears-Haack area distribution, determined as noted above, for each azimuthal plane. The wave drag for a body of revolution of given caliber and length will be minimum if its area distribution is that of a Sears body [3].

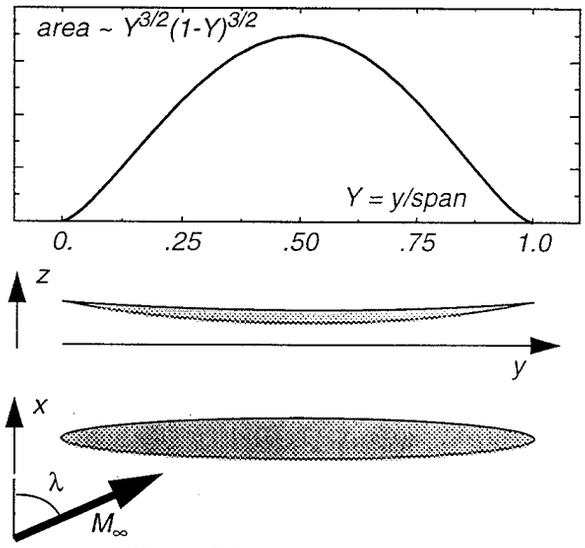

Fig. 1. Oblique flying wing (OFW) in swept high speed flow, with elliptic planform, parabolic bending and a Sears-Haack body section area distribution.

The wave drag of a body of revolution with a given length and base area will be minimum if the area distribution, determined as noted above, is that given by Karman [5], that is, a Karman ogive (see [3]). This corresponds to an elliptic lift distribution. Minimum wave drag requires that all oblique loadings be elliptical. This can be achieved through wing bending as depicted in Fig. 1.

An ellipse has the property that all chord distributions are elliptical. Thus, for each azimuthal plane, an oblique wing with an elliptical spanwise lift distribution will correspond to a Karman ogive. A spanwise elliptic load projects to an elliptic load in the vertical plane and thus also minimizes the induced drag.

Oblique Flying Wing

Nearly fifty years ago R. T. Jones [6], [7] noted that an oblique elliptic wing has the minimum inviscid drag due to lift. As suggested above, this result is more easily derived using Lomax's interpretation of the area rule given by Hayes [8] about the same time. A decade later Smith [9] noted that the Sears-Haack area distribution is the product of an elliptic and a parabolic distribution. Thus, an elliptic wing with a parabolic thickness distribution will have the minimum wave drag due to volume.

We add here for completeness that in a realistic oblique flying wing there is an excess of volume (Rawdon, et al., [10]). As noted earlier, a Sears area distribution minimizes the wave drag due to caliber. This reduces the wave drag to 8/9 that of a Sears-Haack with the same caliber. Thus, for an OFW, a Sears area distribution is more appropriate than a Sears-Haack area distribution, and modest improvements over those reported here for a Sears-Haack area distribution should be possible.

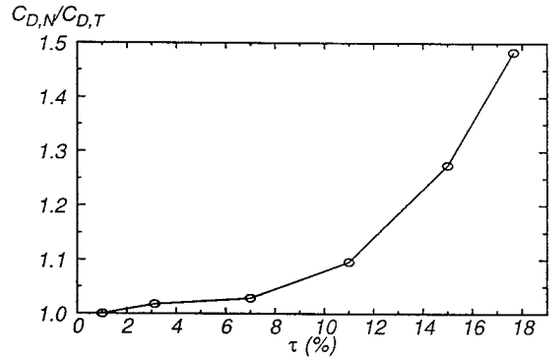

Fig. 2. Ratio of the nonlinear numerical results to linear theory values for the inviscid drag of an oblique elliptic wing with symmetrical cross-sections of the Sears-Haack distribution versus thickness-to-chord. $M_\infty = \sqrt{2}$, sweep angle $\lambda = 60^\circ$.

An oblique elliptic wing simultaneously provides large span and large lifting length. The reduction in the wave drag of an oblique wing comes from being able to provide the optimum distribution of lift and volume in all oblique planes. The aerodynamic advantage of the oblique wing over the swept wing at supersonic Mach numbers stems solely from this fact.

An elliptic wing swept behind the Mach cone will not, however, provide an elliptic load. The downwash will vary nearly linearly down the wing and twist, section thickness variation, or bending must be used on a swept elliptic planform to achieve an elliptic load distribution. Since the section areas are fixed in order to minimize the wave drag due to caliber or volume, twist or bending must be employed. Parabolic bending of the wing provides a linear twist whose magnitude is proportional to $\sin(\lambda)$, providing the mechanism to maintain an elliptic load as the wing's sweep is varied (Fig. 1).

How valid is the linear theory for a realistic OFW? For an oblique elliptic wing with symmetrical cross-sections and a Sears-Haack area distribution, swept to 60 degrees and flying at Mach $\sqrt{2}$, the ratio of the numerical (and nonlinear) to linear theory values for the wave drag due to volume increases rapidly with maximum wing thickness (Fig. 2). This indicates strong nonlinear effects for practical OFWs. The nonlinear effect would be reduced if the sweep angle were increased. Regardless, nonlinear design methods need to be used for the aerodynamic optimization of a realistic OFW.

Shock-free airfoils

At cruise conditions, the flow over an OFW is that behind the nearly conical shock wave emanating from the leading tip. The wing is swept so that the component of this flow normal to the wing's leading edge will be sufficiently subsonic that a thick, shock-free airfoil may be found. We choose a freestream Mach number of $\sqrt{2}$ for simplicity and a sweep angle of 60 degrees for convenience. This gives a normal component Mach number of 0.707, and a spanwise component Mach number of 1.23.

While the flow over this swept OFW is supersonic, the cross-flow plane equations appropriate for an infinite oblique wing (or for a conical flow) are mixed, being hyperbolic outside the bow shock wave and inside the local supersonic cross-flow region, but elliptic elsewhere. Thus, the fictitious gas method (Sobieczky, et al. [11]) for the design of supercritical airfoils was used to design the OFW's cross sections.

For choosing the fictitious equations used in the Euler solver, we prescribe a new energy equation to change the cross-flow equations inside the local supersonic region so that they remain elliptic there (Li, et al., [12]). This results in a shock-free flow with a smooth sonic line, but the wrong gas law, inside the supersonic region. The correct mixed type structure of the transonic flow is recovered in the next step: supersonic flow recalculation by means of the method of characteristics, using the just calculated data on the sonic line for the initial values. This recomputation of the flow with the correct equations of state has a lower density in the supersonic flow and provides a modified, and thinner airfoil design.

It is basically the resulting curvature modifications rather than thickness reduction on the redesigned airfoil that support the resulting shock-free transonic flow. These phenomena and the aerodynamic knowledge base, including the above mentioned supporting theories, have guided us to develop geometry tools with refined shape definition and with options to create parameterized baseline configurations for rapid configuration variations. In the present study the axial volume distribution and the baseline shock-free airfoil determine the requirements for a geometry tool to create suitable input data for design, numerical analysis and optimization.

Geometry generator

New wing design parameters

Aircraft wings are primarily designed on the basis of a planform shape and airfoil data as wing sections. Computer programs that define wings by blending given airfoils for the section distribution along the span have been developed. Mathematical tools are used for surface components of arbitrary aircraft or other aerospace-related configurations. A recent review of this method and its applications is given by Sobieczky [13].

Here we are interested only in the wing component, with additional parameters to be introduced for easier shape control.

Fig. 3 illustrates a spanwise element of an arbitrary wing. The geometrical properties are dominated by the wing section at a given span location. The software developed earlier provided a set of support airfoils which were suitably blended to define wing sections at any span location. Requirements for an OFW, like control of the spanwise volume (wing section area) distribution, and certain flow phenomena observed in earlier numerical modeling (Li, et al., [14]), suggest the need for special mathematical functions to define airfoil shapes of practical interest. These shapes should be controlled with a small set

of parameters. The choice of these functions, and hence the selection of their parameters, was guided by our knowledge of high speed flow phenomena, leading then to a minimum number of needed parameters to efficiently influence flow structure and hence aerodynamic performance of the resulting airfoils.

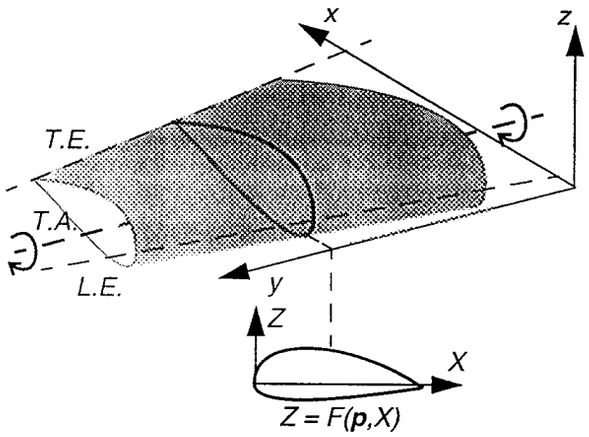

Fig. 3. Definition of the wing surface by planform shape, spanwise airfoil and twist distribution. Airfoil shape is defined by a parameter vector **p**.

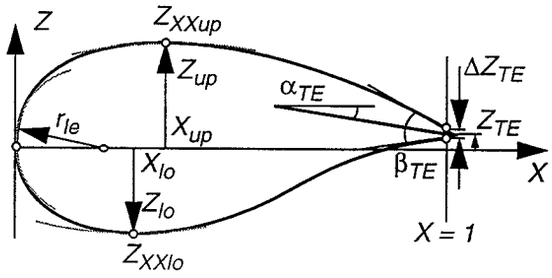

Fig. 4. Basic airfoil geometry is defined by 11 parameters: leading edge radius, upper and lower crest location including curvatures, trailing edge ordinate (at X = 1), thickness, direction and wedge

Fig. 4 shows the selected airfoil function with input of 11 basic geometric parameters. These parameters define the coefficients of polynomials for upper and lower airfoil contours, as can easily be verified:

$$Z = \sum_{n=1}^{6} a_n(\boldsymbol{p}) \cdot X^{n-1/2}$$

Many known classical as well as more sophisticated airfoils can be duplicated by this function with good accuracy; some additional parameters may be introduced for refined shapes of the leading and trailing edges, but these are not used in the present application.

The next step in refining the geometry generator software was replacing the airfoil blending technique by the ability to vary all or a part of the 11 airfoil parameters along span by the same set of basic functions used to piecewise define any arbitrarily complex curve in 3D space. In this first approach of trying to adjust parameters manually, only simple variations to the previously designed shock-free airfoil have been studied. The parameters generated are illustrated in Fig. 5, with data for the generated OFW example to be analyzed in design and off-design conditions as illustrated in the following section.

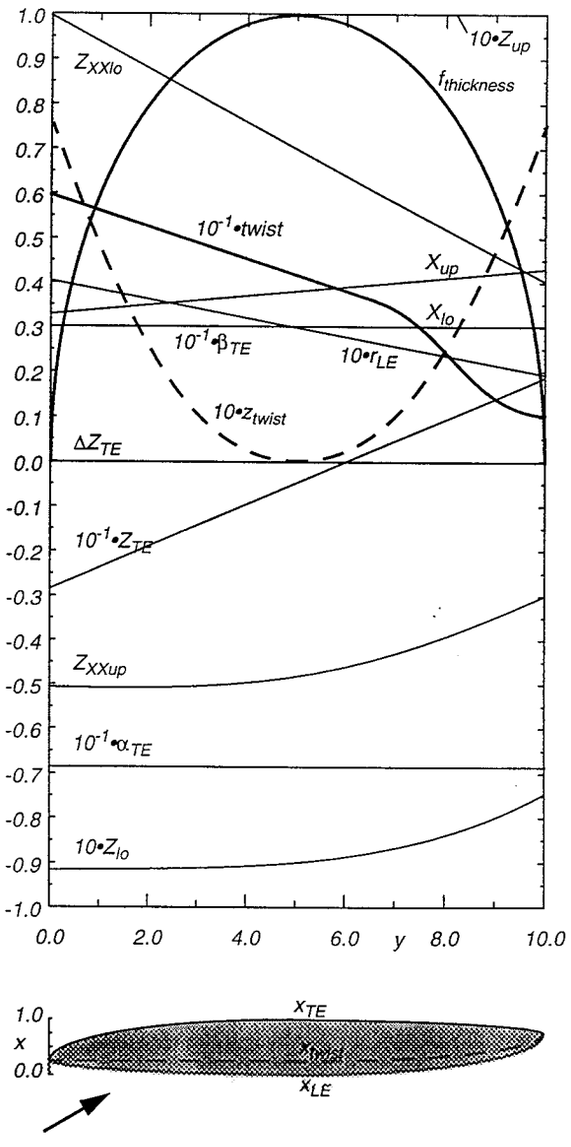

Fig. 5. OFW Wing design parameters and planform as functions of the spanwise direction.

Most parameter variations are basically linear along the span, some of them are just kept constant. But some parameters were modeled by curves. These are further explained here due to their importance for observing constraints prescribed by the previously outlined aerodynamic theories:

Planform and wing twist axis

The basic wing shape is chosen to have an elliptic chord distribution while providing additional sweep back of the trailing portion of the wing. The twist axis is chosen to be the classical quarter chord location; its vertical coordinate, z_{twist}, defines dihedral or bending of the wing. Ellipses and parabolas are used here, requiring only a few data as support input for this software to define function values at any span station.

Thickness factor

For airfoils generated using the 11 input parameters (Fig. 4), their area follows directly from integrating the polynomials for the upper and lower surfaces. Spanwise distribution of this area needs to be tuned as required by the applied aerodynamic knowledge base. For the chosen planform and a constant baseline airfoil its vertical coordinate needs to be multiplied by an elliptic distribution of the thickness factor to model a Sears-Haack area distribution. The physical thickness is then parabolic.

Twist distribution

A very sensitive tool for the control of spanwise aerodynamic load distribution is local section twist. With parabolic wing bending (z_{twist}) providing the majority share of the desired elliptic aerodynamic load, a nonlinear twist distribution, principally along the trailing portion of the wing, allows us to fine-tune the distribution.

Curvature parameters

Nose radius, r_{le}, and crest curvatures, $Z_{xx,up}$, $Z_{xx,lo}$, have been found useful for airfoil design since we have systematic design methods for supercritical transonic wings. With the earlier studies using the single shock-free airfoil in subsonic flow with the Mach number component normal to the leading edge, and the observation that a single airfoil is not enough to generate an OFW with a pressure distribution assumed to be favorable for controlling viscous interaction, variation of the curvature parameters was provided and some early sensitivity studies were carried out.

With the parameters given as functions of span and the spanwise wing sections prescribed by a polynomial, any point of the wing surface can be determined rapidly by function evaluation without iteration and interpolation, which accelerates a global optimization procedure considerably.

Software development

Our first results of the manual input variations confirm the importance of these chosen parameters. The goal is to provide tools and set the stage for an automated numerical optimization procedure for OFWs and other innovative configurations which are not just rescaled versions of existing conventional aircraft. In a toolbox of flexible computer codes for fast predesign studies, we envision preprocessor codes creating 'smart' input data for commercial CAD systems, the latter providing experimental model data as well as computational structured or unstructured grids for CFD simulation. For topologically simple configurations like the OFW without propulsion and control surfaces, the geometry tool also provides structured grids (Fig. 6).

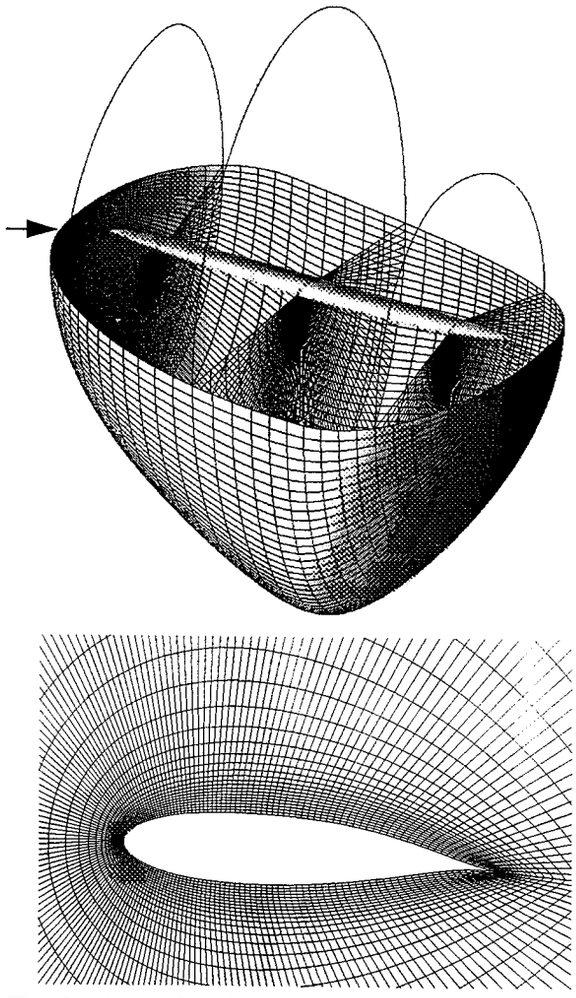

Fig. 6. Algebraic grid with O-O topology: far field boundary (above), center section (below)

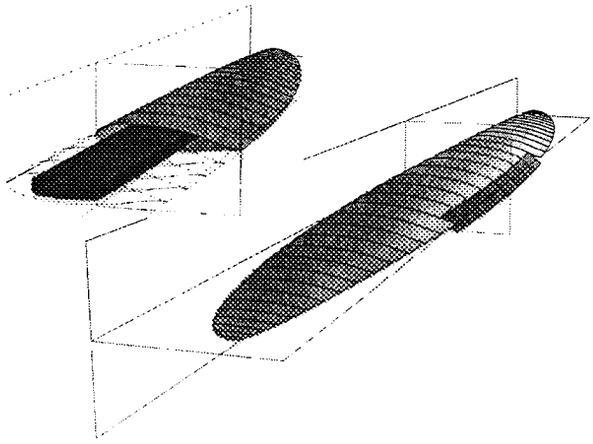

Fig. 7. Geometric modelling of interior structures and control surfaces.

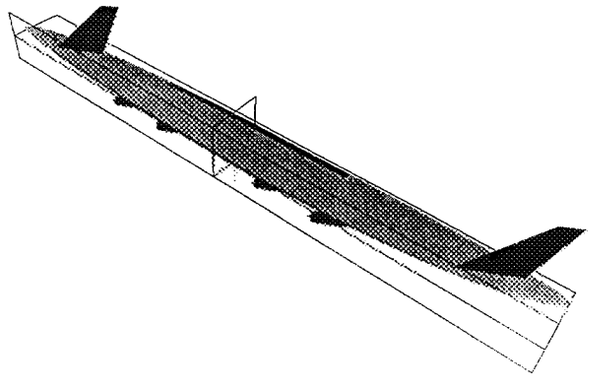

Fig. 8. Oblique Flying Wing aircraft: geometric modelling of the full configuration.

Toward complete parameterized configurations

The present study is aimed at manually designing a wing shape with improved aerodynamic efficiency at given cruise Mach number and sweep angle. This requires configuration generating tools with parameter variations that provide for the control of the most important flow phenomena. The tools used here are precursors to those required for a multidisciplinary study that would includes engines, fins, and flaps. Such a study must consider interior height and volume and also allow for an appropriate structure, (Figs. 7 and 8).

Visualization tools

Regions of influence and dependence in the supersonic flow past an OFW create unusual aerodynamic effects compared to conventional aircraft. These gave rise to some detailed investigation of the occurring 3D shock and Mach wave patterns relative to the wing. Computational methods to visualize shock waves in the flow field as surface elements and characteristics as Mach conoid line traces on the wing help to estimate the regions where geometry parameter changes are required and efficient [15], [16].

Results

Inviscid Optimization

Our design studies utilize the Euler algorithm of the code CFL3D developed at NASA Langley [17]. We use the O-O grid topology shown in Fig. 6. The geometry generator originally used the shock-free airfoil described above as the center section, and then blended varying airfoil sections for a conventional ellipse planform with a 10 to 1 axis ratio.

In our early studies we used twist to achieve an elliptic load distribution and we only endeavored to minimize the drag due to lift, accepting the resulting wave drag due to volume caused by an elliptic (rather than parabolic) thickness distribution (see Li et al., [18]).This resulted in relatively strong cross-flow shock formation on the wing's trailing part, and an unsatisfactory lift-to-drag ratio.

We then used the improved geometry generator to include parametric variations that provide wing bending and a Sears-Haack area distribution. As illustrated in Fig. 5, we prescribe smooth, analytical variations of the set of generating parameters for the mathematical description of wing section coordinates at each span station.

The center section thickness is set at 19%. Tuning of the spanwise airfoil area and thickness factor distribution for the chosen elliptic chord length distribution results in a Sears-Haack volume distribution.

A careful, manual selection of the asymmetrical planform, parabolic bending of the wing and a nonlinear twist distribution are used to achieve a nearly elliptic load distribution. A straight quarter chord line (twist axis) in the leading portion of the wing plane is maintained, but an elliptic shape of its trailing part is chosen. This increases the sweep of the trailing half of the wing.

The numerical analysis at design conditions in inviscid flow is shown in Fig. 9. A supercritical cross-flow pressure distribution is obtained with only moderate

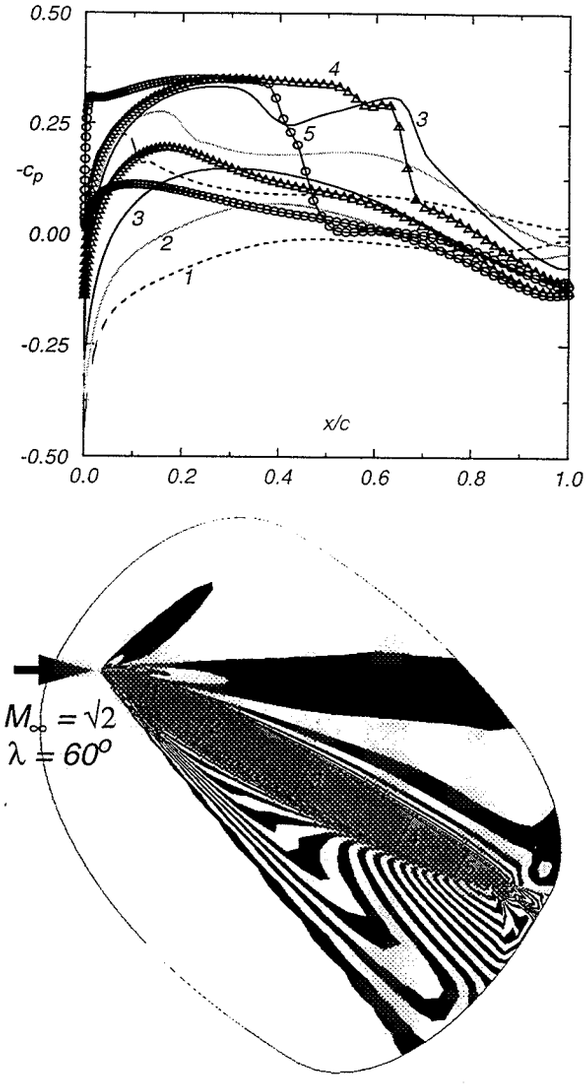

Fig. 9. Pressure distribution in wing plane, 5 grid surfaces and along corresponding 5 wing sections. Cross-flow shock formation occurs along the upper wing surface toward the trailing tip (sections 4 and 5).

cross flow shocks. In a refined analysis of an OFW flow field using our graphic visualization tools for the coalescing characteristics and shock formations, the cross-flow shocks are identified as part of the tail wave reaching upstream to the wing surface, Fig. 10. This indicates that a complete removal of the cross flow shocks on the surface by optimization seems unlikely and reminds us of past efforts to find shock-free airfoils at too high transonic Mach numbers with inverse methods: there so called 'hanging shocks' persist in the flow field even when the flow is shock-free at the airfoil surface. More research needs to be done to investigate the value of such 2D and 3D

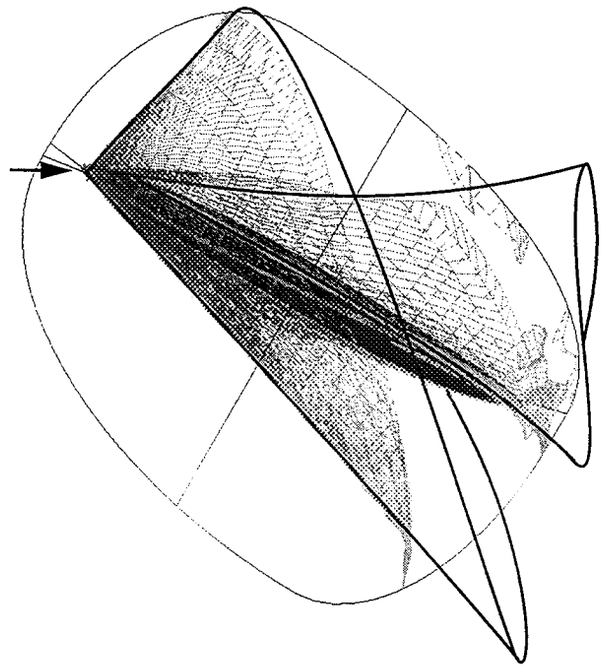

Fig. 10 Visualization of the fore and aft shock conoids

'shock-free' flows, regarding their stability and possible advantages for shock-boundary layer interaction. The wave drag of our OFW is dominated by the more global influence of volume and load distribution. Controlling cross-flow shock strength should be useful in preventing boundary layer separation.

The inviscid L/D of this wing at the design condition is 21.3 at a C_L of 0.145.

We then examined the effect of C_L with fixed sweep on the inviscid L/D, as shown in Fig. 11a. L/D increases slightly to 21.6 as C_L is decreased to 0.125. We then examined the effects of sweep with C_L fixed at 0.135. The results are shown in Fig. 11b. With the sweep increased to 68 degrees, the inviscid L/D increases to 26.3. Next we explored the effect of C_L with the sweep fixed at 68 degrees (Fig. 11c). Lower C_L provided markedly increased L/D. With C_L = 0.0677 we find a maximum inviscid L/D of 35.0. Results for the inviscid flow analysis at $\lambda = 65^o$ are shown in Fig. 12.

The dramatic improvement achieved with increased sweep should not be surprising. With higher sweep, the wing is further from transonic cross-flow effects, effectively thinner, and with its C_L lower, linear theory is more applicable. This then corresponds to a manually optimized nonlinear, but inviscid, design that comes close to providing linear theory results.

Our previous design studies (Li, et al., [14],[18]) sug-

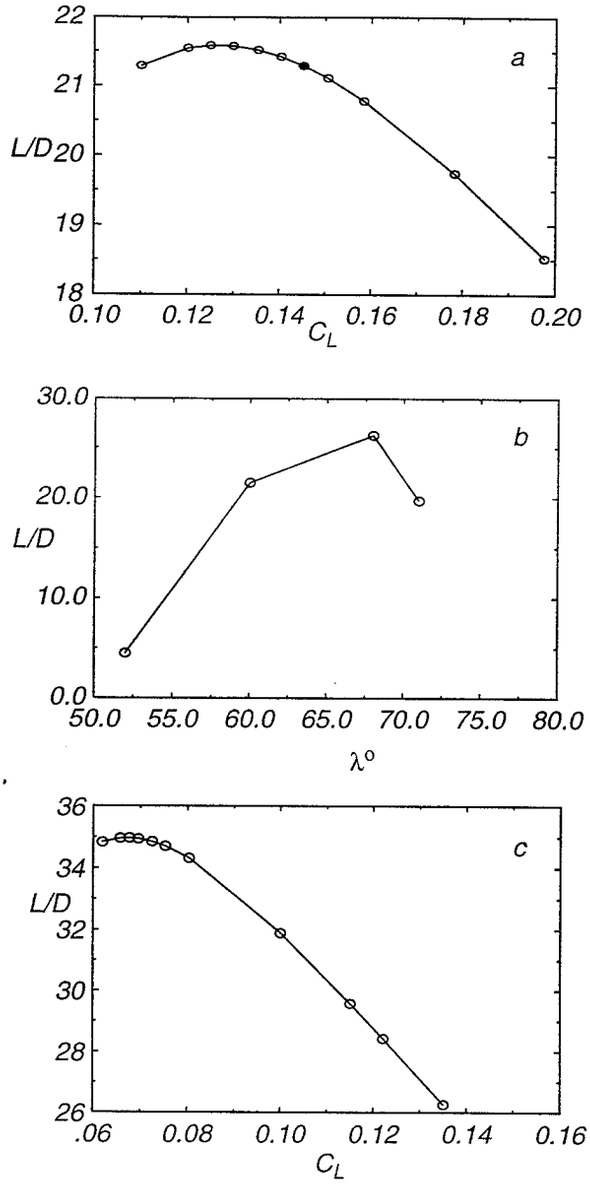

Fig. 11. Inviscid lift-to-drag ratio as a function of lift coefficient and sweep angle.

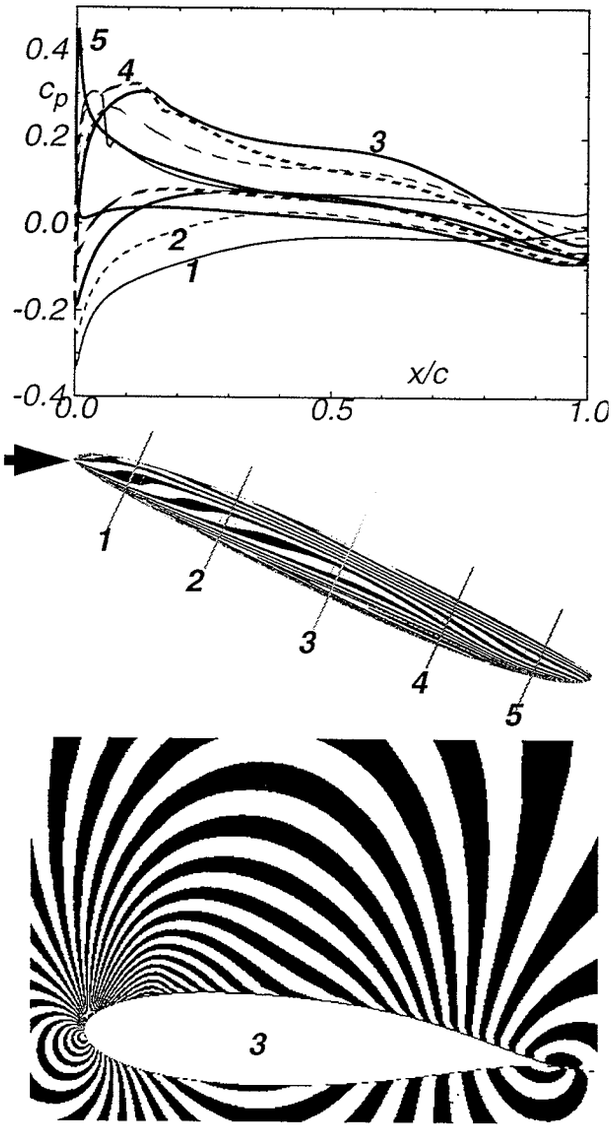

Fig. 12. Pressure distribution at 5 wing sections, Isobars on upper wing surface and in center section plane. $M_\infty = 1.414$, $\lambda = 65^\circ$, $C_L = 0.125$

gested an OFW with a 10:1 axis ratio, a 550 foot span, and a maximum chord of 55 feet. This gave a planform area, S, of 23,758 square feet, and with a thickness of 19% gives a volume of 124,140 cubic feet. Related studies were reviewed by Seebass [19].

To accommodate 800 passengers, the center section thickness was 19% of the chord or 10.5 feet. The studies of Rawdon et al. [10] suggest an estimated takeoff weight of 1.575 million pounds, a weight upon entering cruise of 1.5 million pounds, and a weight upon leaving cruise of 0.9 million pounds.The mid-cruise weight would be 1.2 million pounds.

Viscous optimization

Our OFW should fly at the altitude that, considering viscous effects, maximizes L/D. We may improve L/D by increasing C_L, and incurring a lower inviscid L/D, thereby flying higher and reducing skin friction drag. Because viscous drag = $2q \cdot S \cdot C_F$, where C_F is the average skin friction coefficient, and lift = $q \cdot S \cdot C_L$, we can write for our OFW:

Drag = Lift$\{(D/L)_{inviscid} + 2C_F/C_L\}$,

where C_F is the wing average skin friction coefficient.

Fig. 11c provides L/D as a function of C_L at a sweep of 68 degrees. Given C_L we can find what altitude gives maximum (viscous) L/D. We must first determine the appropriate Reynolds numbers and develop a table of C_F. Here we follow Peterson [20] in applying the method of Sommer and Short [21] to determine the skin friction on a flat plate at supersonic Mach numbers. We assume the wall is adiabatic and use the planform area as the area of the two-sided flat plate for which we compute the viscous drag. The streamwise chord is the mean chord divided by cos(λ). We need an appropriate reference temperature, T', for the boundary layer. Fig. 13 provides C_F as a function of altitude, h. Given the C_L and the weight upon entering cruise of 1.5 million pounds, we can then construct Fig. 14.

The drag-to-lift ratio is a minimum at $C_L = 0.1221$, so we use our analysis of the flow under these conditions to find

$(L/D)_{opt} = \{1/28.423 + 2 \cdot 0.001523/0.1221\}^{-1} = 16.63$, or 16.6 to the accuracy we can determine it. Then ML/D = 23.5. Given the flight altitude of 41,300 feet and C_F, the viscous drag is determined to be 37,420 pounds.

We have reduced inviscid L/D from its maximum of 34.96 to 28.42 to increase C_L and thereby fly higher. Although C_F increases slightly with altitude, the dynamic pressure and thereby skin friction drag are reduced significantly, improving L/D.

Further Optimization

We then reconsidered the effect of sweep and Mach number on L/D and ML/D. For M = 1.414, a sweep of 65 degrees gave an optimum inviscid L/D of 30.287 and a corresponding ML/D of 42.8. An increase in M to 1.5 resulted in a decrease in ML/D to 39.4. From this we conclude that an approximate manual optimum occurs at $M_\infty = \sqrt{2}$, $\lambda = 65^o$, and $C_L = 0.1221$. This reduces the streamwise chord of the wing and increases the average skin friction coefficient to 0.001558, resulting in the viscous L/D given below:

$(L/D)_{opt} =$

$\{1/30.287 + 2\ 0050.001558 / 0.1221\}^{-1} = 17.08$,

with a corresponding ML/D of 24.2.

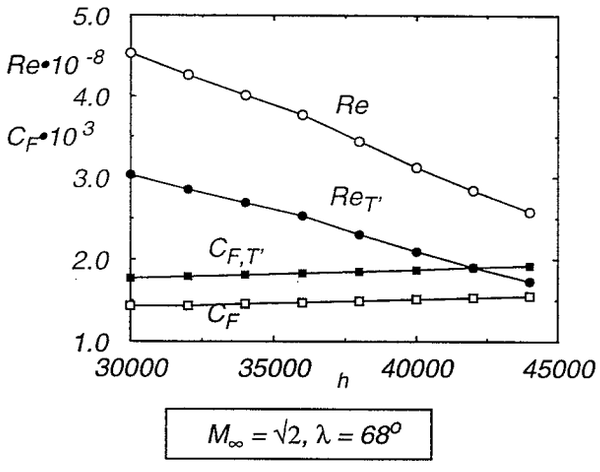

Fig. 13. Reynolds number and skin friction coefficient as a function of flight altitude.

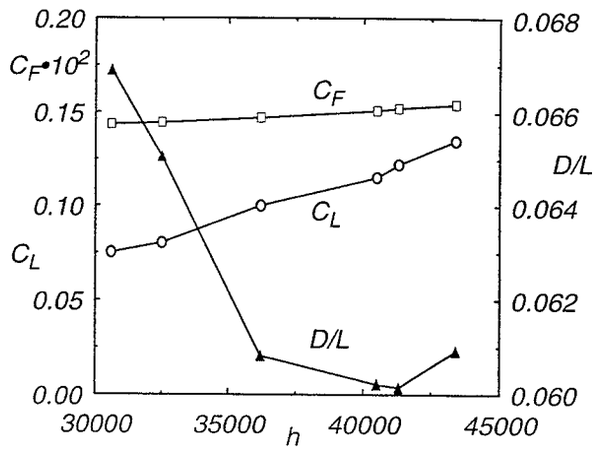

Fig. 14: Lift coefficient, skin friction coefficient and drag-to lift ratio, D/L, as a function of flight altitude.

Linear theory

For these conditions (1.5 million pounds, 41,300 feet, $M_\infty = \sqrt{2}$) linear theory gives a drag due to lift of 28,980 pounds, a drag due to volume of 16,450 pounds, for an inviscid drag of 45,430 pounds and an ideal inviscid L/D of 33.0. The viscous drag is 38,280 pounds and the linear theory drag plus skin friction drag provide an optimum L/D of 17.9 and ML/D = 25.3. Our manually optimized design achieved 17.1. If we had taken a Sears area distribution, the drag due to volume would be reduced by 8/9; this would improves the linear theory L/D to 18.3 (including viscous drag).

During cruise the aircraft climbs to maintain C_L as fuel is burned. For the mid-cruise weight of 1.2 million pounds, the OFW flies at 46,000 feet. At the end of cruise with a weight of 0.9 million pounds, the OFW flies at 52,000 feet.

Off-Design Results

If our OFW weighs 1.575 million pounds on takeoff, achieves $M_\infty = 0.8$ at 1.55 million pounds and $M_\infty = 1.1$ at 1.525 million pounds (based on 5% of fuel to climb to cruise) it will enter cruise at $M_\infty = \sqrt{2}$ at 1.5 million pounds.

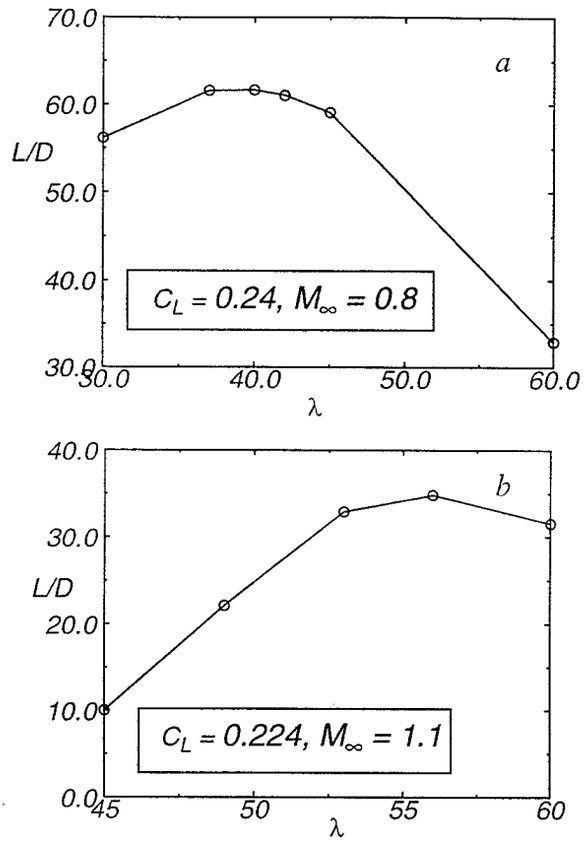

Fig.15. Sweep variation at fixed C_L and M_∞; off-design.

As the candidate OFW accelerates to cruise conditions, its Mach number and altitude are increasing. The wing's sweep that optimizes inviscid L/D is shown in Figs. 15 for fixed C_L.

At Mach 0.8, with the OFW flying at C_L of 0.24, the optimum sweep is 40 degrees and its flight altitude for 1.55 million pounds is 30,800 feet. Under these conditions the OFW achieves the astounding inviscid L/D of 61.7. The corresponding viscous L/D is 31.1 and the ML/D is 24.9. Due to its good transonic performance, the OFW continues to climb to cruise altitude of 41,300 feet while it accelerates to M = 1.1, reducing its C_L to 0.205.

At Mach number 1.1, and with C_L = 0.224, we find the optimum sweep to be 56°. At a weight of 1.525 million pounds, with Mach 1.1, the aircraft will fly at 41,300 feet with C_L = 0.205. We presume then, that at C_L = 0.205, the L/D is at least 35 with $\lambda = 56°$. This corresponds to viscous L/D of 21.5 and ML/D of 23.7. It then accelerates in level flight to its cruise Mach number of $\sqrt{2}$ where L/D is 17.1 and ML/D is 24.2.

Conclusion

With linear theory as a guide, a large OFW was manually optimized to attain an ML/D of 24.2 at the cruise Mach number of $\sqrt{2}$ and altitude of 41,300 feet. This compares well with the linear theory optimum of 25.3. No doubt formal methods could further improve this result. It seems unlikely that designs which exceed the linear theory optimum are possible.

Cruise Mach number was not considered a variable in this optimization. Because of good transonic performance this OFW accelerates through 30,800 feet at M_∞ = 0.8, where its ML/D is 24.9, to M_∞ =1.1 where it has an ML/D of 23.7. As it accelerates to M_∞ =$\sqrt{2}$, the ML/D increases slightly to 24.2.

The remarkable Concorde has ML/D of about 15. The wing designed here achieves 24.1. Without a tail, and assuming the engines are embedded in the wing, this OFW does much better than the Concorde. A very small tail can overcome the small cruise side force, but off-design operations no doubt size the tail. The OFW also does much better off design than the Concorde and would fly efficiently overland at M_∞ = 1.1. At this speed its sonic boom would be refracted and not reach the ground.

Acknowledgments

This work was funded by a NSF CISE Postdoctoral Research Associateship, and DLR basic research funding, TP 336 'Neue Konfigurationen'. Computer support was provided by NASA's Numerical Aerodynamic Simulator program.

References

[1] Lomax, H., "The Wave Drag of Arbitrary Configurations in Linearized Flow as Determined by Areas and Forces in Oblique Planes," NACA RM A55A18, 1955.

[2] Lomax, H., and Heaslet, M. B., "Recent Developments in the Theory of Wing-Body Wave Drag," *J. Aero. S.*, Vol. 23, No. 12, 1956, pp. 1061-1074.

[3] Sears, W. R., "On Projectiles of Minimum Wave Drag," *Quart. Appl. Math.*, Vol. 4, No. 4,1947, pp. 361-366.

[4] Haack, W., "Geschossformen kleinsten Wellenwiderstandes," *Lilienthal-Gesellschaft für Luftfahrt,* Bericht 139, 1941, pp. 14-28.

[5] von Karman, Th. and Burgers, *Aerodynamic Theory,* W. F. Durand ed., Vol. 2, J. Springer, Berlin, 1934, pp. 172-175.

[6] Jones, R. T., "The Minimum Wave Drag of Thin Wings in Frictionless Flow," *J. Aero. Sci.*, Vol 18, No. 2, pp. 1951, 75-81.

[7] Jones, R. T., "Theoretical Determination of the Minimum Wave Drag of Airfoils at Supersonic Speeds," *J. Aero. Sci.* Vol. 19, No. 12, 1952, pp. 813-822.

[8] Hayes, W. D., "Linearized Supersonic Flow," North American Aviation, Report No. AL 222, Los Angeles CA, 1947.

[9] Smith, J. H. B., "Lift/Drag Ratios of Optimized Slewed Elliptic Wings at Supersonic Speeds," *Aeronautical Quart.*, Vol. 12, 1961, pp. 201-218.

[10] Rawdon, B. K., Scott, P. W., Liebeck, R. H., Page, M. A., Bird, R. S., and Wechsler, J., "Oblique All-Wing SST Concept," McDonnell Douglas Contractor Report, NAS1-19345, 1994.

[11] Sobieczky, H., Fung, K.-Y., Seebass A. R., and Yu, N. J., "New Method for Designing Shock-Free Transonic Configurations," *AIAA J.*, Vol. 17, No. 7, 1979, pp. 722-729.

[12] Li, P., Sobieczky, H., and Seebass, A. R., "A New Design Method for Supersonic Transport," AIAA CP 95-1819, 13th AIAA Applied Aerodynamics Conference, San Diego, CA, 1995.

[13] Sobieczky, H., "Geometry Generator for CFD and Applied Aerodynamics," H. Sobieczky ed., CISM Courses and Lectures, No. 366, Springer Wien, New York, 1997, pp. 137-158.

[14] Li, P., Seebass, R. and Sobieczky, H., "The Oblique Flying Wing as the New Large Aircraft," *Proceedings, 20th International Council of the Aeronautical Sciences Congress*, 96.4.4.2, 1996.

[15] Hannemann, M., Sobieczky, H. "Visualization of High Speed Aerodynamic Configuration Design". In: G. M. Nielsen, D. Silver, Proc. Visualization `95, pp. 355 - 358, IEEE Computer Society Press, Los Alamitos, CA, (1995)

[16] Sobieczky, H., and Hannemann, M., "Computational Shock and Mach Waves Visualization Aiding the Development of Aerodynamic Design Techniques," *Proc. 21st Intl. Symposium on Shock Waves*, Gt. Keppel, Australia, 1997.

[17] Thomas, J. L., Taylor, S. L., and Anderson, W. K., "Navier-Stokes Computations of Vortical Flows over Low Aspect Ratio Wings," *AIAA J.*, Vol. 28, No. 2, 1990, pp. 205-212.

[18] Li, P., Seebass, R., and Sobieczky, H., "Oblique Flying Wing Aerodynamics," AIAA 96-2120, 1st AIAA Theoretical Fluid Mechanics Meeting, New Orleans, LA, 1996.

[19] Seebass, A. R., "Oblique Flying Wing Studies," H. Sobieczky ed., CISM Courses and Lectures, No. 366, Springer Wien, New York, 1997, pp. 317- 336.

[20] Peterson, J. B., "A Comparison of Experimental and Theoretical Results for the Compressible Turbulent Boundary Layer Skin Friction with Zero Pressure Gradient," NASA TN-D 1795, 1963.

[21] Sommer, S. C., and Short, B. J., "Free-Flight Measurements of Turbulent Boundary Layer Skin Friction in the Presence of Severe Aerodynamic Heating at Mach Numbers From 2.8 to 7.0," NACA TN 3391, 1955.